Improvement of SCARA robot application in automated blood testing using centrifugation and image processing techniques

Hoang-Dung Nguyen[1,*], Phu-Cuong Pham[1], The-Hien Huynh[1], Tien-Trung Dai[1], Hoang-Dang Le[1] and Hoang-Giang Nguyen[2]

[1]*Faculty of Automation Engineering, Can Tho University, Viet Nam*
[2]*Faculty of Engineering, Kien Giang University, An Giang Province, Viet Nam*
[*]*Corresponding author E-mail: hoangdung@ctu.edu.vn*
DOI: https://doi.org/10.64032/mca.v30i2.395

Abstract

This study proposes an automated system for the blood testing process, specifically the blood centrifugation step, applicable in biomedical engineering. The system reuses the mechanical structure of an existing 4-degree-of-freedom industrial SCARA robot arm while developing additional components, including a vacuum-suction gripper for test tubes, driver circuits for the robotic motors, and dedicated robot control software. Subsequently, the robotic system is integrated with an automated centrifuge and a multi-camera image processing subsystem to create a fully automated blood centrifugation analysis and sample classification platform. Image processing is performed using two camera systems in this study: the first camera system is employed to pick and place test tubes from a specialized tray into the centrifuge machine to separate blood into serum and hematocrit in preparation for the subsequent 'blood test' phase, and the second camera system is used to detect whether the post-centrifugation test tube sample meets the requirements and to associate the data with a patient information label via a barcode on the test tube. The research successfully developed an experimental system, achieving a blood centrifugation cycle time of under 10 minutes per batch and an overall system reliability of 95% during operation.

Keywords: *Automatic system; Blood centrifugation; Image processing; Robotics.*

Symbols

Symbols	Units	Description
$AFOV$	rad	angular field of view
FOV	mm	field of view
s	mm	size of sensor
f	mm	focus length of camera
h	mm	height
H, V	mm	resolution of camera
x, y	cm	position of camera
x_0, y_0	cm	central position of camera
p_h, p_v	pixels	position of tubes/slots
C_ave		average of color
R_i, G_i, B_i		values of Red, Green, Blue
n		sum of pixels

Abbreviations

SCARA	Selective compliance assembly robot arm
TCP/IP	Transmission control protocol/Internet protocol
EtherCAT	Ethernet for control automation technology
OpenCV	Open computer vision library
GUI	Graphic user interface
RBC	Red blood cells
RGB	Red green blue

1. Introduction

Blood testing plays a pivotal role in the prevention, diagnosis, and management of chronic diseases, informing over 70% of clinical decisions and enabling early detection of conditions such as diabetes, cardiovascular disorders, and malignancies [1, 2]. Central to this process is blood centrifugation, which separates whole blood into distinct components as plasma, platelets, white blood cells, and red blood cells based on differences in specific gravity, thereby facilitating accurate downstream analysis of biomarkers, including microRNAs critical for disease profiling [3]. Beyond routine serum and plasma preparation, centrifugation supports advanced applications such as concentrating platelet-rich plasma (PRP) for regenerative medicine, isolating hemoglobin for biochemical studies [4], and removing unwanted cellular elements in therapeutic contexts [5]. Standardized protocols, including centrifugation at 3,000–4,000 RPM for 5–15 minutes, are essential to ensure analyte stability and the integrity of results [6, 7].

Despite the critical role of blood centrifugation in clinical diagnostics, conventional manual methods remain fundamentally limited by their labor-intensive nature, susceptibility to human error, and inherent time constraints. Manual processes such as tube loading, rotor balancing, post-centrifugation visual inspection of separation quality, and subsequent rack sorting, which expose laboratory staff to biohazards, elevate the risk of sample mix-ups or mislabeling, and require operators to remain tethered to rigid centrifuge cycles, often resulting in prolonged turnaround times and reduced throughput in high-

Received: 22 November 2025; Revised: 6 January 2026; Accepted: 25 February 2026.

volume hospital settings [8]. Moreover, previous studies have consistently demonstrated that variability in centrifugation parameters (speed, duration, and centrifugal force) significantly affects the accuracy of results, including electrolyte measurements and other diagnostic analytes, whereas repeated manual runs suffer from poor inter-run consistency due to operator-dependent factors [9, 10, 11]. The large daily sample volumes processed in clinical laboratories further exacerbate these issues, as operator fatigue, inter-technician variability, and reliance on individual expertise introduce systematic inconsistencies and increase error rates [12]. Although partial automation of sample preparation, phlebotomy, or downstream analysis has been proposed to improve uniformity and reliability [13], most prior efforts have focused on isolated stages rather than achieving full end-to-end automation of the centrifugation workflow itself.

To address these challenges, automation of the blood centrifugation process emerges as a transformative solution. By integrating robotic systems, such as SCARA manipulators for precise tube handling, and advanced image processing for real-time quality assessment, automated platforms minimize human intervention, reduce processing time, and enhance reproducibility. Similar to robotic applications in minimally invasive surgery, such systems decouple operators from repetitive tasks, enabling asynchronous workflows where samples are loaded, centrifuged, inspected, and sorted without constant supervision [14, 15]. Intelligent barcode tracking, EtherCAT-controlled centrifugation, and camera-based evaluation of plasma separation further ensure traceability, precision, and safety.

This study introduces a fully automated blood centrifugation system designed to streamline laboratory workflows by:

- Employing a the mechanical structure of a four-degree-of-freedom SCARA industrial robot (Model: EPSON SRC-320 ABS, Japan), which is further integrated with additional sensors, a PLC controller, and AC servo motor drivers (Mitsubishi MR-J3, Japan) to control the robot's degrees of freedom and form a complete robotic system into the centrifugation procedure to optimize pick-and-place operations, reducing manual labor and processing time;
- Leveraging Basler cameras and Python-based image processing to identify red blood cell and plasma regions using image processing techniques, as abnormal variations in these regions are associated with altered physiological conditions or pathological states in humans [16];
- Implementing EtherCAT and TCP/IP protocols in PLCs and the computer for high-speed, reliable device communication. The communication system is capable to perform multiple tasks, including sample loading and unloading on racks, transfer of samples into the centrifuge, automatic configuration of centrifugation parameters (e.g., rotational speed and centrifugation time), identification of red blood cell and plasma regions after centrifugation, and real-time updating of sample-related information in a laboratory management software system

By automating the most repetitive and error-prone phase of blood testing, this system significantly shortens analytical turnaround, improves diagnostic reliability, and supports scalable, high-throughput clinical laboratories.

2. Problem statements

The blood centrifugation process, conducted in accordance with medical requirements, consists of three main stages, detailed as follows:

Stage 1. Before centrifugation: The blood centrifugation process begins after blood samples are collected from patients, with each sample labeled with a barcode to distinguish and manage patient information, thereby preventing sample mix-ups and reducing the risk of errors during testing and result reporting. The samples are then transported to the laboratory. There, medical staff perform the blood centrifugation process to prepare for blood testing. Upon arrival at the laboratory, the blood samples are placed in foam or plastic trays to secure them and prevent shaking during transport. Upon receiving the samples, staff verify the number of samples to determine the total number requiring centrifugation, then proceed with the centrifugation steps.

Stage 2. In centrifugation, the blood centrifugation process begins with collecting and labeling blood samples with barcodes to prevent mix-ups and errors, followed by their transport to the laboratory, where medical staff pick and place them in foam or plastic trays to ensure stability during transfer between the trays and a centrifugation machine. In the lab, samples are processed in batches of 6 to 32 tubes, depending on the centrifuge machine capacity, with each batch requiring an even number of tubes arranged symmetrically for balance. The total number of tubes determines the number of batches, and the first cycle maximizes tube placement, while the final batch, if short of tubes but even, maintains symmetrical arrangement; if odd, a counterweight tube (a previously centrifuged tube or one with equivalent mass) is added to ensure an even number for balanced centrifugation, enhancing accuracy, efficiency, and reducing processing time and errors. The centrifugation time and speed vary depending on the medical facility or clinic, as different regulations apply. However, a general recommendation is to centrifuge at 3,000 to 4,000 RPM for 5 to 10 minutes to ensure successful blood separation [7, 17]. After securing the centrifuge lid, the centrifugation process is initiated.

Stage 3. After centrifugation: After the centrifugation process is complete, the medical staff open the centrifuge lid, remove the blood samples, and visually assess the blood's condition to determine if the separation was successful. The blood is then classified into three categories: successfully separated blood, unsuccessfully separated blood, and hemolyzed blood. Successfully separated blood is characterized by complete separation into plasma and red blood cells, with plasma appearing as a clear, pale yellow liquid comprising approximately 50-60% of the total volume [18, 19], and the remaining portion consisting of dark red blood cells. Hemolyzed blood, while separated into two distinct layers, exhibits red-colored plasma resulting from the rupture of red blood cells due to various factors. Successfully separated blood samples are transferred to another tray for further testing, while hemolyzed samples prompt the medical staff to request a second blood sample collection.

The proposed automated system addresses these limitations by integrating a SCARA robot with dual vision-based control systems and advanced communication protocols. Real-time position identification of blood tubes and empty slots on the tray is achieved via the first camera system, which captures

images, applies an estimated position algorithm, and transmits precise coordinates to the PLC for seamless robot control, enabling fast, accurate pick-and-place operations without manual intervention. Moreover, the opening and closing of the centrifuge lid are facilitated by a pneumatic cylinder with a throttle valve to adjust speed and a 5/3 valve to control the lid's open and closed states, eliminating operator dependency during loading and unloading. Finally, a key advancement in the automated centrifugation system is the replacement of manual visual inspection by medical staff with the camera-based quality assessment of blood samples post-centrifugation. The second camera identifies barcodes to retrieve patient information, then evaluates the blood separation state via color analysis, generating a binary (PASS/FAIL) output that enables the robot to sort the tubes onto trays based on their separation status. The entire system operates automatically and synchronously via a robust PLC-computer communication system to accelerate the overall centrifugation cycle and substantially enhance laboratory efficiency, sample integrity, and diagnostic workflow reliability.

3. Automated blood test system design

3.1 Drive circuit and control software design for robotic arm

The robotic system for blood sampling and testing in Fig. 1 integrates several key components to ensure efficient, precise, and safe operation. The robot's mechanical structure is reused from an existing 4-degree-of-freedom industrial SCARA robot. Whereas the power electronics (driver circuits) and control software were entirely designed and developed by the research team at the Department of Automation Engineering, Can Tho University. Specifically, the computer serves as the central hub for managing and controlling the entire system. It also provides signals from the image processing system to the PLC for picking-and-placing operations, offering a user interface for programming the robot and monitoring its activities. The PLC directly handles control and navigation functions based on sensors and operators, actuators, valves, and other devices, while feeding system status back to the computer and implementing safety protocols. Drivers convert PLC signals into precise commands for the robot's movement and control the suction manipulator as motors and pneumatic solenoid valves, facilitating seamless interactions among components. Push buttons provide operators with essential controls to initiate, halt, or adjust specific robot functions. Limit switches define and enforce operational boundaries to safeguard personnel and equipment. Proximity sensors mounted on the conveyor belt detect blood trays at both input and output points. Negative pressure sensors monitor the suction cup's status to prevent blood tube drops or failed pickups, ensuring reliable operation. The robot executes pre-programmed tasks as transportation, assembly, inspection, or material handling, interacting with its environment via sensors and controls to fulfill assignments. Finally, a 24V power supply energizes the control system, supporting overall functionality in the blood sampling and testing workflow.

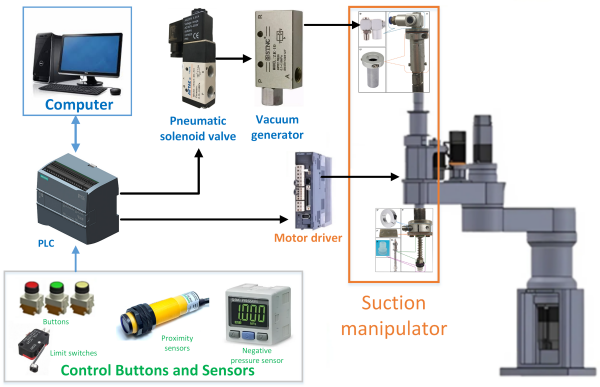

Figure 1: The robotic system for blood tubes sampling and testing.

3.2 Centrifugation based blood test

The blood centrifugation system, as illustrated in Fig. 2(a), comprises several key components and functions for automated operation. In Fig. 2d, the Siemens S7-1200 PLC (PLC1) serves as the central manager and controller for the entire robotic and centrifuge system, acting as the master in communication processes. The Omron NX1P2 PLC (PLC2) controls and guides the centrifuge, managing the high-speed motor, pneumatic valves for cylinder actuation, reading position sensor signals to determine cylinder status, and verifying the centrifuge's home position to enable return-to-home functionality. The advanced motion driver converts PLC2 signals into precise control commands for the servo motor, regulating its speed and position as desired. Cylinder auto switches provide feedback on cylinder positions to the PLC2 for state recognition, while metal proximity sensors establish the home position for the centrifuge during position-controlled operations. A power supply delivers electricity to the whole system. Due to the centrifuge rotor's design in Fig. 2b, which positions blood tubes at a 45° angle relative to the horizontal plane, contrasted with the SCARA robot's vertical Z-axis movement at 90° to the horizontal, a mechanical system is required to automatically adjust the centrifuge base's tilt angle, facilitating accurate tube placement and retrieval by the robot. The centrifuge's weight is concentrated on the vertical clamp and transmitted to the bearings, enabling efficient lifting and lowering operations. Position adjustments by elevation are achieved through the integration of a throttle valve and cylinder position sensors Fig. 2c, which provide real-time feedback for the centrifuge's lifting process.

3.3 Image processing system

The image processing system utilizes two cameras to capture images and transmit them to a computer via USB, shown in Fig. 3. On the computer, image processing algorithms from the OpenCV library, implemented in Python, are employed to analyze the data. The data from Camera 1 is processed to determine the coordinates for picking up blood tubes and placing them on the tray. Meanwhile, Camera 2 is tasked with recognizing barcodes on the tubes to update patient information and identify successfully centrifuged blood tubes. The successfully centrifuged blood tube consist of separated components by density: the heavier red blood cells settle at the bottom, the lighter plasma forms the top layer, and a thin "buffy coat" of white blood cells and platelets is in the middle [20]. The

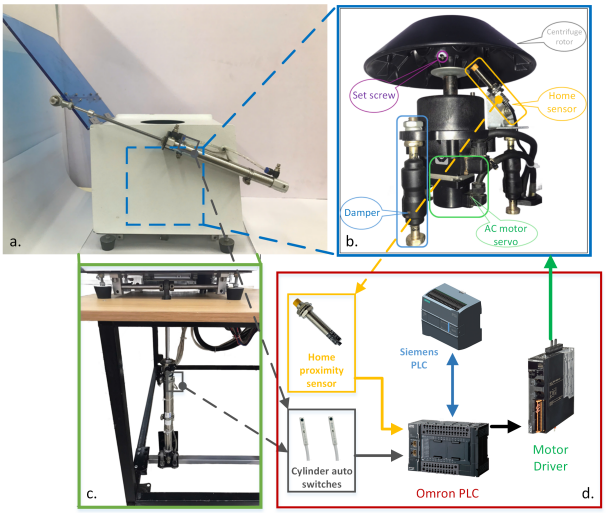

Figure 2: The automated blood tubes centrifuge system (a); the centrifugal spinnning machine (b); the lifting system (c); the centrifuge control and communication system (d).

operations of both cameras are sequentially processed based on control signals from the PLC to the computer for image analysis. The processed results are then sent back to the PLC1, enabling the robot to sort the tubes onto the tray and categorize them as either meeting or failing the separation standards. The image processing system is divided into three main functions: determining the positions of picking tubes and placement holes on the tray from image pixels; identifying barcodes to manage patient information; and identifying the status of centrifugal blood tubes, handled through the following algorithms.

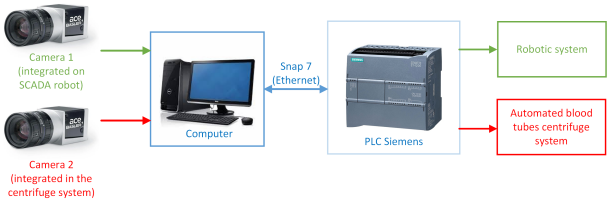

Figure 3: The multi-cameras image processing system.

3.4 Communication system

The communication architecture, comprising programmable logic controllers (PLCs) and a central computer, is illustrated in Fig.4. PLC1 serves as the master controller managing the operations of the robotic arm and vacuum suction manipulator while continuously monitoring the system's states throughout the process. PLC2 interfaces with PLC1 via EtherNet/IP to relay real-time status updates for the blood tube centrifuge subsystem. To facilitate this interoperability, the LCCF_EnetAdapter library [21] converts Profinet signals to EtherNet/IP, ensuring high precision and rapid response times. Additionally, PLC1 establishes a direct connection with the computer via its IP address. This linkage is implemented using the Snap7 Python library [22], enabling seamless bidirectional communication. The computer, in turn, interfaces with the camera systems for image acquisition, transmits command signals to PLC1, and receives comprehensive system state data to dynamically update the graphical user interface (GUI) and monitor process progress.

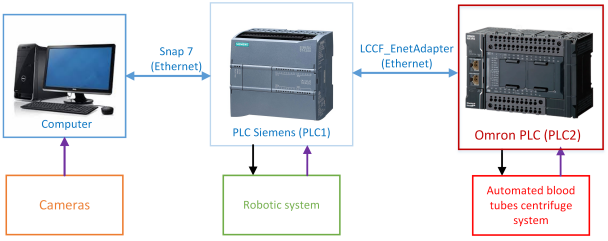

Figure 4: The communication system in this study.

4. Methodology

4.1 Determine positions for picking and placing tubes on the tray by Camera 1

Based on the scale calculation Eq. (1) from pixels to real position coordinates in [23], the conversion from camera pixels to practical coordinates uses Eqs. (2)–(5).

$$Scale = (Scale_h, Scale_v) = \left(\frac{FOV_h}{H}, \frac{FOV_v}{V}\right) \tag{1}$$

$$AFOV_h = 2\tan^{-1}\left(\frac{s_h}{2f}\right) \tag{2}$$

$$AFOV_v = 2\tan^{-1}\left(\frac{s_v}{2f}\right) \tag{3}$$

$$FOV_h = 2h\tan\left(\frac{AFOV_h}{2}\right) \tag{4}$$

$$FOV_v = 2h\tan\left(\frac{AFOV_v}{2}\right) \tag{5}$$

where $AFOV_h$ and $AFOV_v$ (rad) are the angular field of view on horizontal and vertical scale, FOV_h and FOV_v (mm) are the field of view on horizontal and vertical scale, s_h, s_v is the horizontal and vertical size of sensor, f is the focus length of the camera, h is the height of from the camera to the plane of the object detection. The camera's resolution is $H \times V$. The image processing method for position determinations in Fig. 5 begins with resizing images captured by Camera 1, followed by applying a median blur (11×11) and a Gaussian blur (5×5) to reduce noise and enhance the edges of the test tube tray. A threshold technique isolates the left and right white tray edges, allowing calculation of the tray's four corners. To compute coordinates accurately, the image resolution should be between 1.3×10^6 and 1.41×10^6 pixels. Using these corners, extraneous areas are filtered, leaving only the tray with test tubes or empty slots.

The next step involves the Canny Edge and Hough Circle algorithms [24, 25] to detect circular shapes within the tray image. The positions for picking or placing tubes are determined by analyzing the color thresholds of areas with and without tubes, based on the detected circle colors. In this study, the coordinate system $x\mathbf{O}y$ is chosen as the global coordinate system, attached to the robot base in Figs. 6a. and 6b.; $x_c\mathbf{C}y_c$ is the coordinate system attached to the camera; the $x_{Im}\mathbf{O}_{Im}y_{Im}$ is the coordinate system attached to the captured image. The tube coordinates are calculated based on Eq. (6) and Eq. (7), then sent

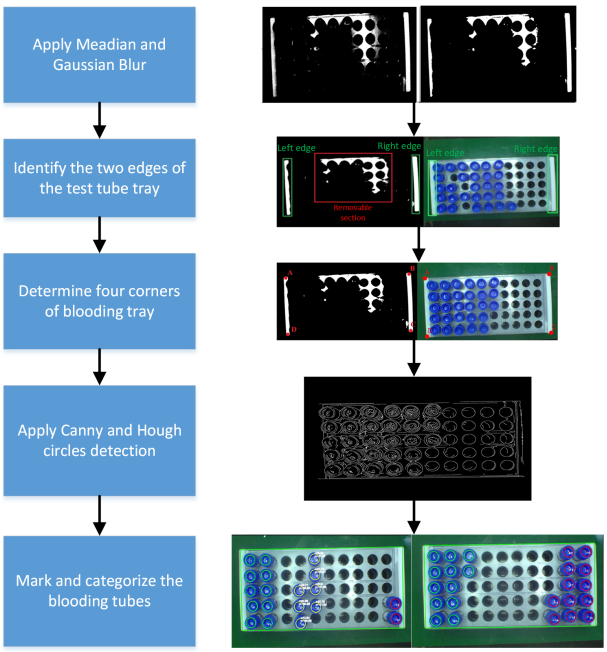

Figure 5: Position determination algorithm for picking and placing tubes on the tray by Camera 1.

to the PLC1 to control the robot arm for pick-and-place during the centrifugation and post-centrifugation sorting processes.

$$x = \text{round}(x_0 + Scale_h \times (H/2 - p_h), 3)(\text{cm}) \quad (6)$$

$$y = \text{round}(y_0 + Scale_v \times (V/2 - p_v), 3)(\text{cm}) \quad (7)$$

where x_0 (cm), y_0 (cm) are the central position coordinate $\mathbf{C}(x_0, y_0)$ on the xy plane of the camera at the capturing position, p_h, p_v are the position in pixels of the tubes/slots on the captured image. The values are desribed by the Fig. 6.

When tubes arrive at pre-centrifugation staging, the robot rearranges them and marks completed tubes: green for those meeting standards, red for failing, and yellow for uncentrifuged. After centrifugation, Camera 2 evaluates results. Tubes with acceptable samples go in the outermost left slot (top to bottom); those with unacceptable samples go in the opposite slot (bottom to top).

The Home point is near the drop-off location at the recognition station, presented in Fig. 6c. , marked by a single dark circular hole with a low color range [20, 30, 30] and a high color range [180, 255, 255]. To recalibrate, the system checks deviation from the image center to the Home point. If the offset exceeds 0.25 cm, a new Home coordinate is sent to the PLC1; otherwise, no recalibration is needed. To enable precise execution of pick-and-place tasks, the robotic arm relies on image processing methods that use data from Camera 1, in combination with an automatic calibration procedure. This reliance ensures that the coordinate positions estimated by Camera 1 are accurately interpreted and executed by the robot.

4.2 Barcode and centrifuged blood sample identification on a tube by Camera 2

To read the barcode on the test tube, the barcode image is clarified by applying a threshold filter. And then the information is recognized by encoding with the pyzbar library [26]. If the test tube lacks a barcode, the recognition result is returned as failed. To detect the outline of the test tube, the thresholded image is processed using contourArea to identify the tube's contours. The output consists of contours, which are a list of detected contours, where each contour is an array containing coordinate points (x_i, y_i)that form the boundary.

For analyzing successful centrifugation based on the separation of red blood cells (RBCs) and plasma, excess portions of the test tube are removed based on corresponding color thresholds (low [0, 0, 0], high [180, 255, 80]). The RBC portion is defined as the black-colored region with the color coordinates (low [0, 0, 0], high [180, 255, 80]). The remaining portion of the test tube constitutes the plasma. If the number of contours for both the RBC and plasma portions is exactly one each, the process proceeds to the next step.

In this step, average color values are computed to define the differences between passing and failing results. The average color is calculated by dividing the total sum of pixel colors by the total number of pixels as Eq. (8). Based on experimental results, the identified color of the plasma region is defined within the RGB range (R: 35–45, G: 115–135, B: 30–35). If the plasma color values fall within this range and the blood in the test tube is distinctly separated into two portions (RBC and plasma), the centrifugation result is deemed to meet the standards.

$$C_{ave} = \left(\frac{\sum_{i=1}^{n} R_i}{n}, \frac{\sum_{i=1}^{n} G_i}{n}, \frac{\sum_{i=1}^{n} B_i}{n} \right) \quad (8)$$

where R_i, G_i, B_i are the values of Red, Green, and Blue in the RGB color space at the ith pixel, respectively; n is the sum of pixels in the contour. The image process of Camera 2 is summarized by Fig. 7.

5. Experiment results and discussion

The proposed automated blood centrifuge consists of robotic, centrifuged, image processing systems, and supports as buttons and conveyers belt, presented in Fig. 8.

5.1 Operation process

The entire automated workflow of the system in Fig. 9 is divided into four steps designed to achieve efficient, contacless handling and quality: sequentially picking up six blood tubes and placing them into the centrifugation chamber (**Step 1**); picking up blood tubes and depositing them into the inspection chamber (**Step 2**), then checking the centrifuged blood status in the chamber (**Step 3**); and retrieving blood tubes from the inspection chamber and placing them back into the tray (**Step 4**).

The process begins with the robot moving to the blood tray, activating the light to enhance image contrast, enabling the vision system to accurately localize blood tube positions, as described in **Stage 1**a. Subsequently, the light is turned off, and the robot moves to the blood tube position, lowers the Z-axis, activates pneumatic suction, and picks up the tube, as shown in **Step 1**b. The robot raises along the Z-axis to remove the blood tube from the tray, as illustrated in **Step 1**c, followed by moving the tube to the centrifuge loading position before releasing the suction to deposit it, as depicted in **Step 1**d. This cycle repeats until all six tubes are symmetrically loaded. Upon completion of the centrifugation cycle (performed under controlled speed and duration to ensure optimal plasma, hematocrit separation),

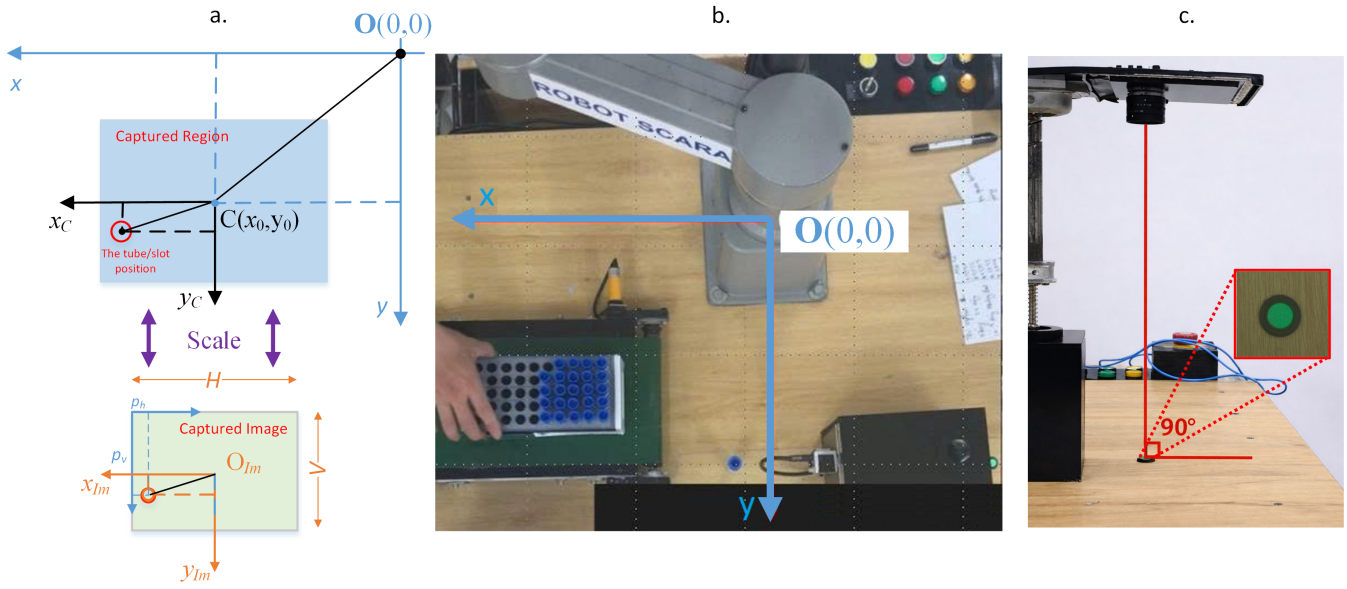

Figure 6: The image processing implementation for controlling the robot in pick-and-place operations: a. the transformation model between the robotic coordinate system and the camera coordinate system; b. the robotic coordinate system attached to the base of the robot arm; c. the Home position.

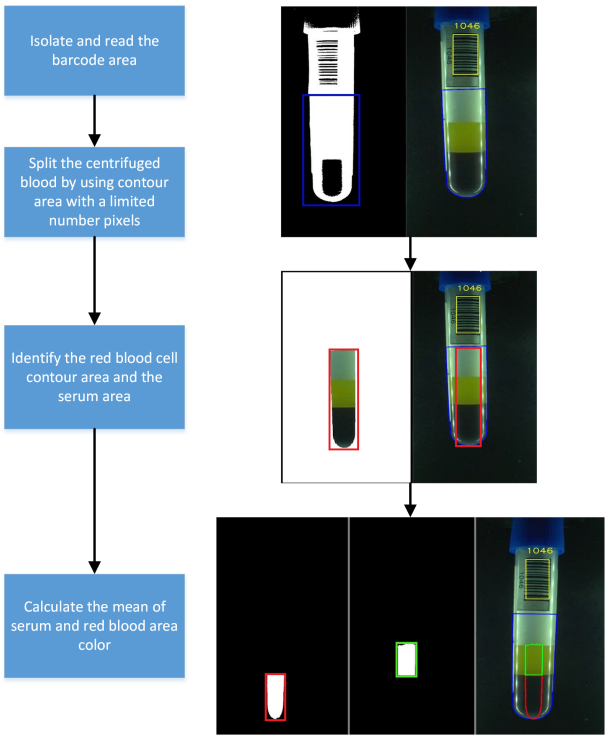

Figure 7: Barcode and centrifuged blood sample identification algorithm.

the robot returns to the centrifuge. It lowers the Z-axis and activates pneumatic suction, as shown in **Step 2**a. Next, the Z-axis is raised to remove the blood tube from the centrifuge, as illustrated in **Step 2**b, after which the robot moves to the home position, turns on the light to identify the home positions, as described in **Step 2**c. The robot then adjusts its position and lowers the Z-axis to insert the centrifuged tube into the inspection chamber, as shown in **Step 2**d.

Once the Z-axis is lowered into the inspection chamber, the suction cup holding the blood tube rotates to allow Camera 2 to recognize the tube. If the plasma and red blood cell layers meet the satisfactory separation, the tube is marked as PASS, as shown in **Step 3**; otherwise, it is marked as FAIL (e.g., hemolysis, incomplete separation, or abnormalities). In the current work, the focus is on the two clearly distinct layers that form after centrifugation. Fig. 8 shows straw-colored plasma, accounting for less than 55%, within the normal range. That can vary depending on hydration status, sex, and individual variation [16]. After recognition, the Z-axis rotation is stopped, and the tube is raised out of the inspection chamber.

The robot then conveys the assessed tube back to the tray to determine the placement location, as shown in **Step 4**a. The robot then proceeds to the starting position on the tray and arranges PASS tubes from top to bottom, as described in **Step 4**b. Conversely, FAIL tubes are directed to a separate region and arranged from bottom to top to facilitate subsequent re-sampling or re-testing, as in **Step 4**c. Placement is completed by lowering the Z-axis to partially insert the tube into the slot before deactivating the vacuum gripper, as depicted in **Step 4**d.

5.2 GUI design for automated blood test

The graphical user interface for system control is designed in WinCC, enabling users to monitor the system's current status during the blood testing process. The interface, as illustrated in Fig. 10, is divided into four key information sections:

- **System Status:** This provides details such as the operational state (RUNNING or COMPLETED) via lamp signals.
- **System Operation Phase:** This displays the system's current status within one of the three main phases (PHASE 1: Picking tubes to the centrifuge system, PHASE 2: Blood tube analysis PHASE 3: Classify blood tubes) of the automated centrifugation process, which are further subdivided into seven smaller sub-processes (1. Raising/ Lowering the centrifuge base; 2. Opening/ Closing the cap of the centrifuge; 3. Home position; 4. Centrifuged; 5.

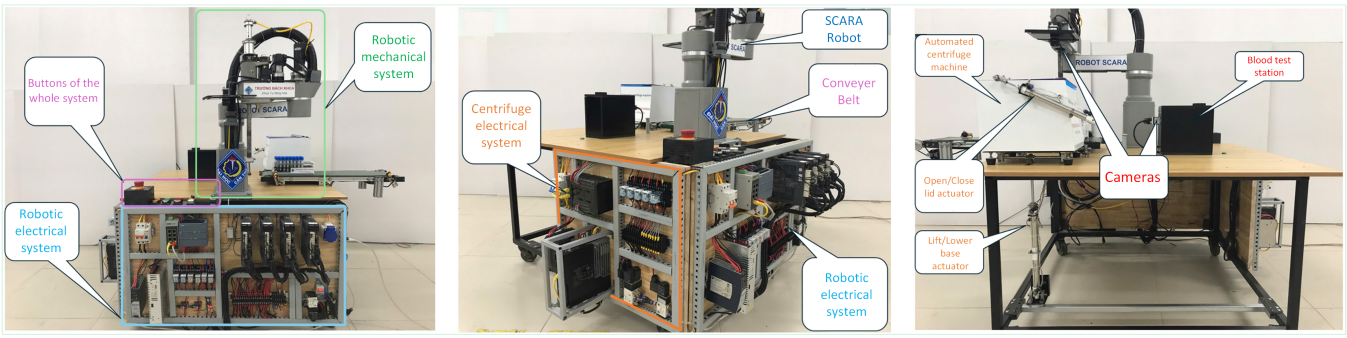

Figure 8: The proposed automated blood centrifuge system.

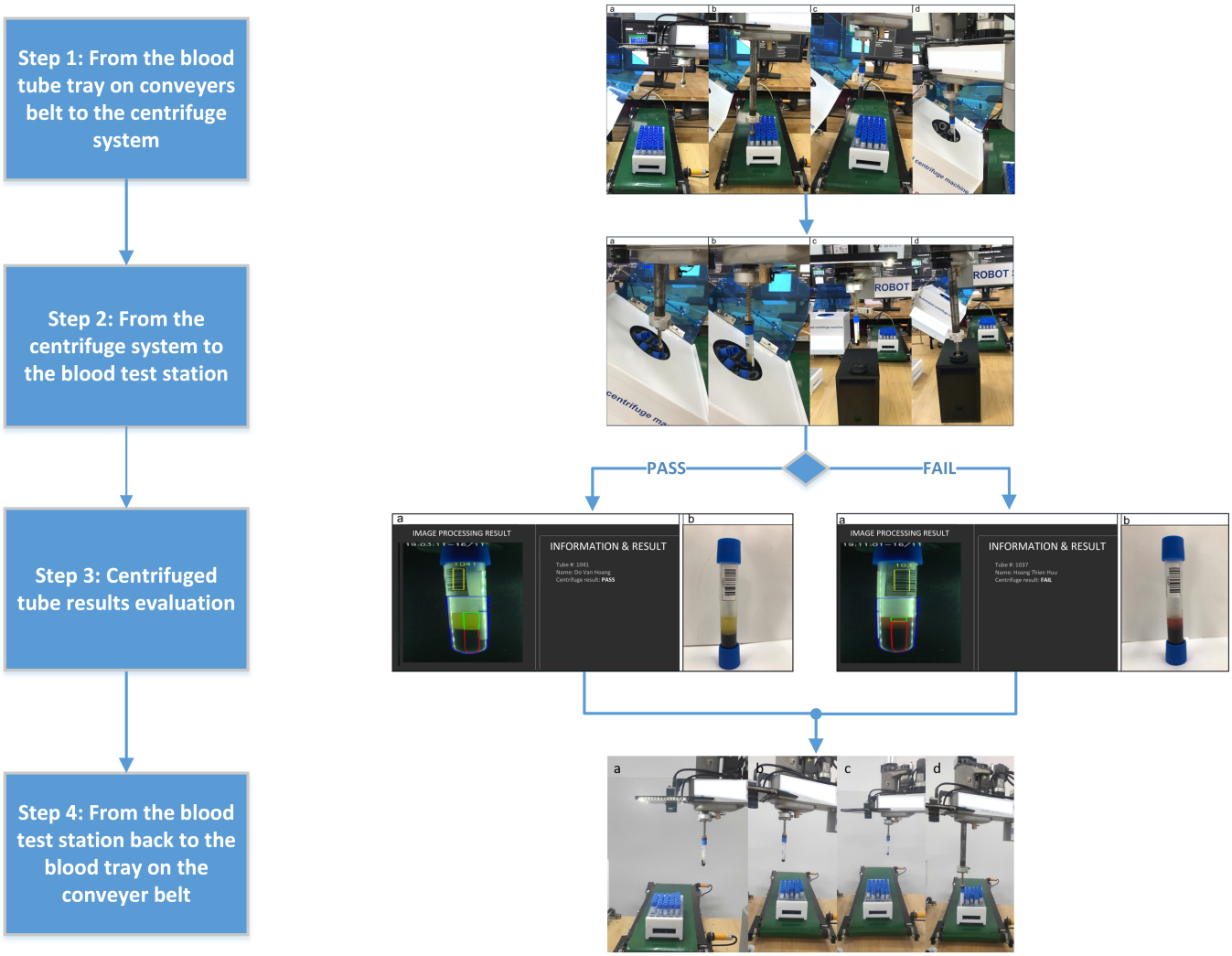

Figure 9: The experimental process results.

Position calibrated; 6. Conveyer belt and 7. Suction cup). Throughout the operation, if an error occurs, the system automatically issues an Error alert and halts functioning.

- **Process Operating Parameters:** This shows the system's parameters, the number of test tubes to be picked from the tray into the centrifugation chamber, the number of blood tubes currently in the centrifugation chamber, the total number of FAIL tubes, and the PASS tubes.

5.3 Discussion

The blood samples used in the experiments are obtained from members of the research team. To assess the success rate of each process, five trials (4 batches for each trial and 6 blood sample tubes for each batch) have been deployed in our current experiment. To evaluate the system's reliability at each step, a step was rated as PASS if completed, and FAIL if an error occurred or the step could not be finished. The outcomes from each step were used to assess overall system reliability via the following expression:

$$R = A \times B \times C \times D \tag{9}$$

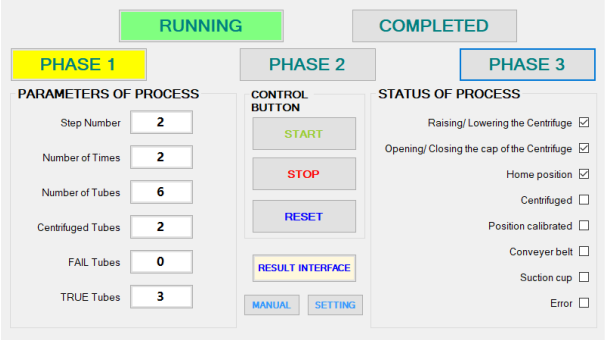

Figure 10: The GUI control design in this study.

where R, A, B, C, and D represent Boolean values indicating the reliability of the system, **Step 1**, **Step 2**, **Step 3**, and **Step 4**, respectively. The system's reliability is based on Eq. (9), which is illustrated in Fig. 11. The results demonstrate strong overall stability and reliability of the proposed automated system. The average precision across all 20 batches reaches 95.0%, indicating that the integrated SCARA robot, dual-camera vision guidance, PLC coordination, and auto-calibration mechanism collectively ensure highly consistent performance. Notably, 15 out of 20 batches (75%) achieved precision at 100%, reflecting robust repeatability when mechanical and environmental conditions remain stable.

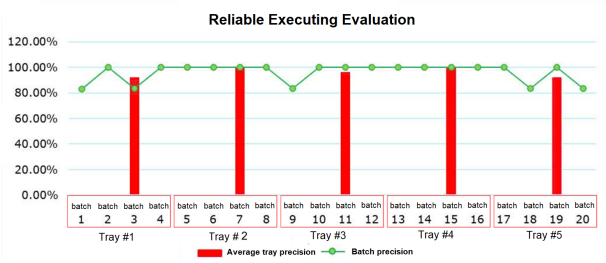

Figure 11: The system's reliability of execution.

Throughout execution, time is recorded to evaluate the efficiency of the automated procedure. Timing starts when a signal is received from the sensor at the end of the conveyor belt. It ends when the last test tube is placed into the test tube tray from the inspection chamber. Figure 12 presents the execution time evaluation of the automated blood centrifugation system across 20 consecutive batches. These batches are grouped into five trays, with processing times ranging from approximately 9.5 to 11.5 minutes per batch. Moderate fluctuations are observed. The time starts high at around 11.5 minutes for the initial batches. It dips to about 10 minutes in mid-trays and gradually trends downward toward 9.5-10 minutes by the final batches. This suggests potential system stabilization or minor optimizations over repeated cycles. The most time-consuming steps in each batch are image processing for real-time position estimation using Camera 1 and quality assessment using Camera 2. These require computational analysis of tube coordinates, barcodes, and color-based separation. Centrifugation itself, the fixed-duration spin cycle essential for plasma-hematocrit separation, also contributes significantly. Together, these steps account for the bulk of the observed durations. The system's average time is 10.61 minutes. Efficiency can be further enhanced by increasing the robot's operational speed, thereby accelerating pick-and-place operations, tray transfers, and auto-calibration routines, all without compromising precision or reliability.

The proposed system is designed to address the problems mentioned in Section 2. It can reduce human errors, ensure robust PLC operations, and provide a stable time cycle and reliability. Reduce labor by using a fully automated system in the centrifugation workflow and managing patient information. Moreover, manual/semi-automation requires multiple devices and consequently more laboratory space than full automation, thereby limiting the free movement of operators among devices [27]. Finally, the system can control the centrifugation speed for further testing, as reported in [7]. It also has a reasonable cost, based on the reused robotics system and popular PLCs, compared to the expensive robotic systems, as [28] notes.

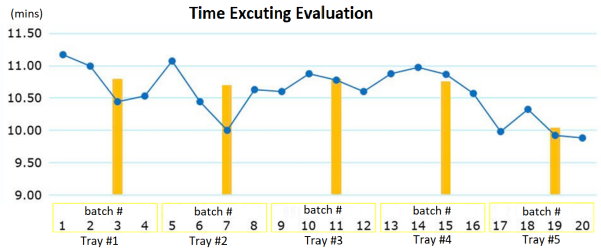

Figure 12: The time execution process evaluation.

6. Conclusion

This study successfully designed and implemented an automated robotic system for blood centrifugation in laboratory testing, achieving a precision rate exceeding 95% for the entire system, as shown in Fig. 11. The SCARA robot capabilities were enhanced through the integration of a vacuum suction gripper and a camera-based system for accurate position detection and blood tube manipulation. The automated workflow is structured into three primary phases: initial grasping of the test tube for centrifugation, retrieval of the centrifuged tube via the blood analysis recognition subsystem, and sorting of the tubes into designated regions on the holder to facilitate subsequent processes. The centrifuge itself incorporates a camera system for precise detection of plasma and erythrocyte separation. Furthermore, the system features a robust mechanical framework that supports seamless end-to-end automation, encompassing sample intake from the conveyor belt, centrifugation, analysis, and return to the belt for iterative processing. Finally, the image processing module effectively classifies blood tubes into successful (well-separated) and abnormal (e.g., hemolyzed) states, while also determining tube positions on the tray and holder for optimized handling. Beyond these demonstrated strengths, the system holds substantial potential for further improvement in future research: accelerating overall throughput by increasing robot joint speeds and optimizing motion trajectories, reducing image processing latency through GPU acceleration, or extending automation to upstream phlebotomy or downstream biochemical analyzers. These enhancements could position the platform as a scalable, high-efficiency solution for modern clinical laboratories, ultimately improving diagnostic turnaround, staff safety, and operational cost-effectiveness.

Acknowledgement

We would like to thank Can Tho University supporting for this work. We thank P. H. Dang, T. D. Son, and N. H. Phuoc for their assistance in sample preparation and data analysis.

References

[1] D. Weatherby, & S. Ferguson, "Blood chemistry and CBC analysis: clinical laboratory testing from a functional perspective", Vol. 4, *Weatherby & Associates*, LLC, 2002.

[2] A. Zhang, H. Sun, & X. Wang, "Serum metabolomics as a novel diagnostic approach for disease: a systematic review", *Analytical and bioanalytical chemistry*, vol. 404, no. 4, pp. 1239-1245, Sep. 2012, doi: 10.1007/s00216-012-6117-1.

[3] X. H. Zheng , C. Cui, X. X. Zhou, Y. X. Zeng, & W. H. Jia, "Centrifugation: an important pre-analytic procedure that influences plasma microRNA quantification during blood processing", *Chinese journal of cancer*, vol. 32, no. 12, pp. 667, Dec. 2013, doi: 10.5732/cjc.012.10271.

[4] C. T. Andrade , L. A. Barros, M. C. P. Lima, & E. G. Azero, "Purification and characterization of human hemoglobin: effect of the hemolysis conditions", *International journal of biological macromolecules*, vol. 34, no. 4, pp. 233-240, Aug. 2004, doi: 10.1016/j.ijbiomac.2004.05.003.

[5] N. Al-Saedi, M. Agarwal, W. Ma, S. Islam, & Y. Ren, "Proteomic characterisation of lupin (Lupinus angustifolius) milk as influenced by extraction techniques, seed coat and cultivars", *Molecules*, vol. 25, no. 8, pp. 1782, Apr. 2020, doi: 10.3390/molecules25081782.

[6] A. Colak, B. Toprak, N. Dogan, & F. Ustuner, "Effect of sample type, centrifugation and storage conditions on vitamin D concentration". *Biochemia medica*,vol. 23, no. 3, pp. 321-325, Oct. 2013, doi: 10.11613/BM.2013.039.

[7] F. I. Allison, A. C. Ojule, L. Shittu, & E. O. Bamigbowu, "The effects of speed and duration of centrifugation on the values of some commonly measured plasma electrolytes", *European Journal of Medical and Health Sciences*, vol. 2, no. 2, Apr. 2020, doi: 10.24018/ejmed.2020.2.2.187.

[8] W. Godolphin, K. Bodtker, D. Uyeno, & L. O. Goh, "Automated blood-sample handling in the clinical laboratory", *Clinical chemistry*, vol. 36, no. 9, pp. 1551-1555, Sep. 1990, doi: 10.1093/clinchem/36.9.1551.

[9] M. Lebl, "Centrifugation based automated synthesis technologies", *JALA: Journal of the Association for Laboratory Automation*, vol. 8, no. 3, pp. 30-35, Jun. 2003, doi: 10.1016/S1535-5535-04-00267-9.

[10] C.J.O. Bacal, J.W. Maina, H.H. Nandurkar, M. Khaleel, R. Guijt, Y. Chang, K.M. Dwyer, and L.F. Dumée, "Blood apheresis technologies - a critical review on challenges towards efficient blood separation and treatment", *Materials Advances*, vol. 2, no. 35, pp. 7210-7236, Nov. 2021, doi: https://doi.org/10.1039/D1MA00859E.

[11] M.H. Fallatah, A.F.A. Otaibi, R.R. Aljohani, W.J. Ghabban, A.A. Alshehri, "Evaluation of Centrifugation Technique and the Effect of Centrifugation Condition on the Laboratory Samples", *Journal Of Healthcare Sciences*, vol. 4, no. 12, pp. 1003-1009, 2024, doi: 10.52533/JOHS.2024.41248.

[12] S.C. Gupte, "Automation in Blood Centre: Its impact on Blood Safety", 'Asian journal of transfusion science, vol. 9, no. 1, pp. S6-S10, Apr. 2015, doi: 10.4103/0973-6247.157016.

[13] Y. Hou, R. Mishra, Y. Zhao, J. Ducrée, J.D. Harrison, "An Automated Centrifugal Microfluidic Platform for Efficient Multistep Blood Sample Preparation and Clean-Up towards Small Ion-Molecule Analysis", *Micromachines*, vol. 14, no. 12, pp. 2257, Dec. 2023, doi: 10.3390/mi14122257.

[14] M. L. Balter, A. I. Chen, A. Fromholtz, A. Gorshkov, , T. J. Maguire, & M. L. Yarmush, "System design and development of a robotic device for automated venipuncture and diagnostic blood cell analysis", In *2016 IEEE/RSJ international Conference on intelligent Robots and systems (IROS)*, pp. 514-520, Oct. 2016, doi: 10.1109/IROS.2016.7759102.

[15] M. L. Balter, J. M. Leipheimer, A. I. Chen, A. Shrirao, T. J. Maguire, & M. L. Yarmush, "Automated end-to-end blood testing at the point-of-care: Integration of robotic phlebotomy with downstream sample processing", *Technology*, vol. 6, no. 02, pp. 59-66, 2018, doi: 0.1142/S2339547818500048.

[16] J.J. Bjerre-Bastos, C. Sejersen, A.R. Bihlet, N.H. Secher, A.L. Mackey, C.C. Kitchen, ... & H.B. Nielsen, "An estimate of plasma volume changes following moderate-high intensity running and cycling exercise and adrenaline infusion", 'Frontiers in Physiology, vol. 13, no. 948087, Jul. 2022, doi: 10.3389/fphys.2022.948087.

[17] M. Quirynen, S. A. M. Siawasch, J. Yu, & R. J. Miron, "Essential principles for blood centrifugation". *Periodontology 2000*, vol. 97, no. 1, pp. 43-51, May. 2025, doi: 10.1111/prd.12555.

[18] P. Gupta, "What your blood tells? A review", *Journal of Cell and Tissue Research*, vol. 20, no. 2, pp. 6897-6913, 2020.

[19] A. Kaplan,"Preparation, Storage, and Characteristics of Whole Blood, Blood Components, and Plasma Derivatives", *Transfusion Medicine*, Mar. 2021, doi: 10.1002/9781119599586.ch5.

[20] J. Mathew, P. Sankar, & M. Varacallo, "Physiology, Blood Plasma", *StatPearls Publishing, Treasure Island (FL)*, Apr. 2023.

[21] "Application example: EtherNet/IP Adapter for SIMATIC", *Siemens*, 2025.

[22] B. Zheng, J. Xu, H. Li, J. Xing, H. Zhao, & G. Liu, "Development of remotely monitoring and control system for siemens 840D sl NC machine tool using Snap 7 codes", In 2017 2nd *International Conference on Electrical, Automation and Mechanical Engineering (EAME 2017)*, pp. 108-112. Atlantis Press, Apr. 2017, doi: 10.2991/eame-17.2017.26.

[23] X. Yang, & S. Fang, "Effect of field of view on the accuracy of camera calibration", *Optik*, vol. 125, no. 2, pp. 844-849, Jan. 2014, doi: 10.1016/j.ijleo.2013.07.089.

[24] E. A. Sekehravani, E. Babulak, & M. Masoodi, "Implementing canny edge detection algorithm for noisy image", *Bulletin of Electrical Engineering and Informatics*, vol. 9, no. 4, pp. 1404-1410, 2020, doi: 10.11591/eei.v9i4.1837.

[25] W. Hou, "Research on automatic hole making technology of industrial robot based on Hough circle detection algorithm", *International journal of wireless and mobile computing*, vol. 24, no. 3-4, pp. 352-360, Jun. 2023, doi: 10.1504/IJWMC.2023.131325.

[26] L. Hudson, "pyzbar (Version 0.1.9) [Python package]", *Python Package Index*, url: pypi.org/project/pyzbar/, Accessed: 2022

[27] J. Cid, N. Comasòlivas, A. Pérez-Aliaga, N. Illingworth, & M. Cardoso, "Comparison of automated versus semi-automated whole blood processing systems: A systematic review", *Vox Sanguinis*, vol. 118, no. 4, pp. 263-271, Jan. 2023, doi: 10.1111/vox.13400.

[28] M. A. Jeraiby, J. M. Moshi, S. A. Dar, M. M. Habibullah, M. Yahia, , S. E. B. Abdalla, ... & N. S. Burayk, "Comparative Evaluation of Centrifugation Speed and Its Impact on Diagnostic Accuracy", *Journal of Clinical Laboratory Analysis*, vol. 29, no. 23, pp. e70120, Oct. 2025, doi: 10.1002/jcla.70120.